Application of a machine learning in predicting bearing capacity of ring foundation in anisotropic clays

Dang Khoa Nguyen[1], Trong Phuoc Nguyen[1,×], Van Qui Lai[2]

[1] Faculty of Civil Engineering, Ho Chi Minh City Open University, 97 Vo Van Tan Street, Ho Chi Minh City, Vietnam
[2] Faculty of Civil Engineering, Ho Chi Minh City University of Technology (HCMUT), VNU-HCM, Ho Chi Minh City, Vietnam
[×]Corresponding author: phuoc.nguyen@ou.edu.vn

Abstract. A novel equation is proposed to predict the bearing capacity of ring foundation embedded in anisotropic clays using a machine learning approach: Multivariate adaptive regression spline (MARS). The previous study's numerical results are adopted as the MARS model's training data. The results from the proposed equation are compared with previous studies and field data. As a result, a good agreement between results from the proposed equation and those from previous studies is obtained. The findings of this research can be a valuable tool for calculating the stability number of ring foundations in anisotropic clays.

Keywords: Machine learning, Ring foundation, Anisotropic clays

1 Introduction

Ring footings, which support axisymmetric structures like offshore platforms, silos, and chimneys, are a popular choice for foundation systems because they are more cost-effective than circular footings but have similar efficiency. To examine the effectiveness of ring footings, studies have been conducted on their bearing capacity on both sand and clay [1-4]. Various calculation methods for estimating the bearing capacity of ring footings have been developed, including numerical models such as FLAC and finite element analysis (FEA) with the Plaxis code. Previous researches have also used finite element limit analysis (FELA) to estimate the bearing capacity factors for ring foundations on cohesive-frictional soils. Besides, a number of studies have investigated the bearing capacity of ring footings on soils or rocks, including researches by Khatri and Kumar, Lee et al., Yang et al., Birid and Choudhury, Yodsomjai et al., Lai et al., and Keawsawasvong et al. [5-16].

The strengths of anisotropic clays were first mentioned by Casagrande and Carillo [17] and Lo [18]. Ladd [19, 20] proposed relations between undrained shear strengths obtained from tri-axial compression, tri-axial extension, and direct simple shear and the plasticity index of clay. Krabbenhoft and Lyamin [21] proposed a new failure criterion for anisotropic clays called the anisotropic undrained shear failure criterion.

Non-homogeneous clays have an increase in shear strengths with depth, which is important in geotechnical stability issues [22-28]. The coupling effect of anisotropic and non-homogeneous behaviors of undrained soils is investigated in various works such as excavation [30–33], tunnel [34-36], slope stability [29,30], trapdoors phenomena [31-33], and foundation capacity [34-37].

However, predicting the ultimate bearing capacity and failure mechanism of a ring foundation embedded in anisotropic and non-homogenous clay is still limited.

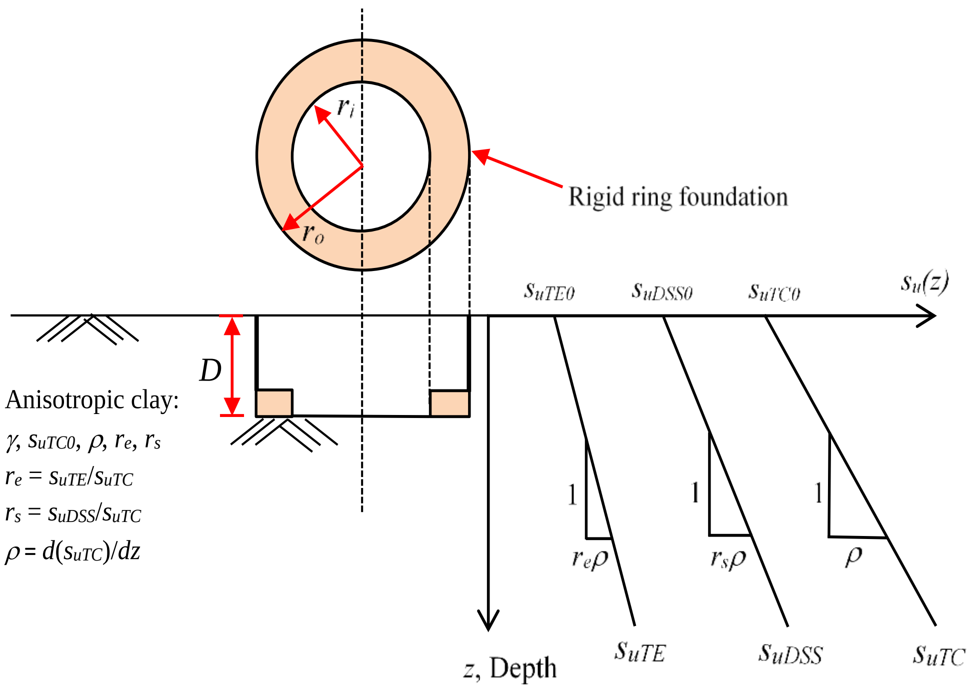

Fig. 1. Problem definition of a rigid ring footing embedded on anisotropic and heterogeneous clays.

Multivariate adaptive regression splines (MARS), a part of machine learning, has become an increasingly popular approach in various fields such as construction management, building materials, and geotechnical analysis. However, there is a lack of research on using MARS for predicting the bearing capacity of ring foundations in anisotropic and non-homogeneous clay.

The new equation for determining the bearing capacity factor of ring footings embedded in anisotropic and non-homogeneous clays is constructed using the MARS model in this study. The bearing capacity is examined by considering the dimensionless bearing capacity factor and several input variables, including inner and outer radius, embedded depth, an increase of shear strength gradient, and three undrained shear strengths.

2 Problem definition

The problem of a ring footing embedded in anisotropic and non-homogeneous clays is depicted in Figure 1. The rigid ring footing, defined by an inner radius r_i, outer radius r_o, and an embedded depth D, experiences a uniform pressure (q) on its rough interface with the soil. The circular shape of the footing is reasonable for the axisymmetric model.

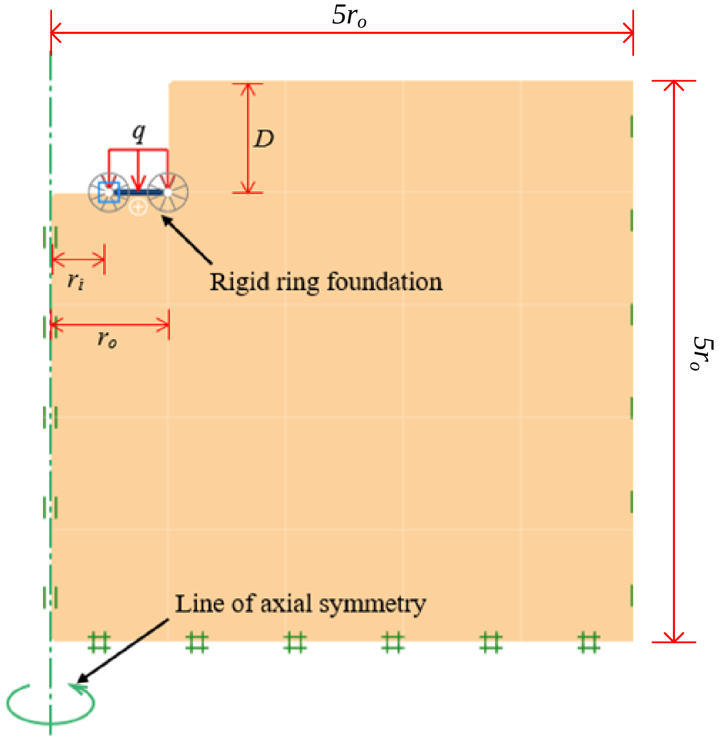

Fig. 2. Numerical model of a rigid ring footing.

The soil in this study is considered weightless to ignore the effect of unit weight on undrained bearing capacity results. Also, it is assumed to be perfectly plastic following the AUS failure criterion. The model considers three anisotropic undrained shear strengths, obtained from tri-axial compression (s_{uTC}), tri-axial extension (s_{uTE}), and direct simple shear (s_{uDSS}). These parameters are normalized using the $r_e = s_{uTE}/s_{uTC}$ and $r_s = s_{uDSS}/s_{uTC}$ ratios, and their relationship $r_s=2r_e/(1+r_e)$, which is proposed by Krabbenhoft and Lyamin [21] and Krabbenhoft et al [22]. Krabbenhoft et al. [22] showed that r_e value is from 0.5 to 1, and Fig. 3 illustrates the effect of this parameter on the yield surface of the AUS failure criterion. When $r_e = 1$, meaning that $s_{uTC} = s_{uTE} = s_{uDSS}$, the AUS failure criterion [22] turns into the Tresca failure criterion.

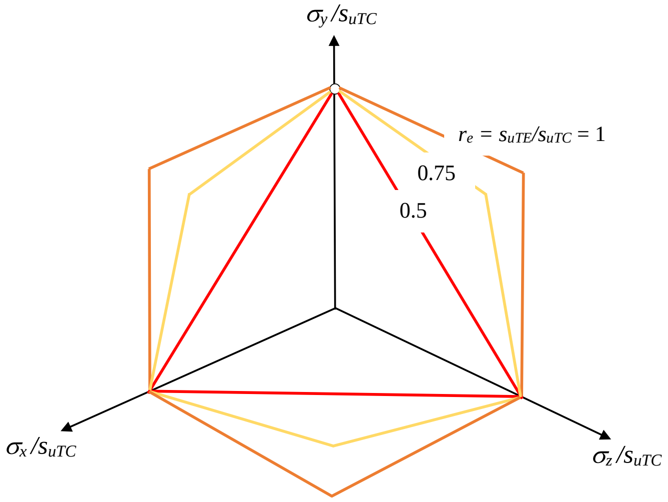

Fig. 3. Generalized Tresca surface used in the Anisotropic Undrained Shear (AUS) failure criterion (Krabbenhoft and Lyamin 2015; Krabbenhøft et al. 2019).

The non-homogeneous characteristics of clays are described by three undrained shear strengths with increasing depth, as shown in Eqs. (1-3).

$$s_{uTC}(z) = s_{uTC0} + \rho z \tag{1}$$

$$s_{uTE}(z) = s_{uTE0} + r_e \rho z \tag{2}$$

$$s_{uDSS}(z) = s_{uDSS0} + r_s \rho z \tag{3}$$

where s_{uTC0}, s_{uTE0}, and s_{uDSS0} are shear strength values at the ground surface and ρ presents the increasing of shear strength with depth z. Furthermore, q is a linear gradient of undrained shear strength. The value of q can be determined through tests such as vane shear or CPT.

Butterfield's dimensionless approach [38] is used to reduce the number of input parameters, and four critical dimensionless inputs are investigated: r_i/r_o, D/r_o, r_e, and $m=\rho r_o/s_{uTC0}$.

$$N = \frac{q}{s_{uTC}} = f\left(\frac{r_i}{r_0}, \frac{D}{r_0}, r_e, m = \frac{\rho r_0}{s_{uTC0}}\right) \tag{4}$$

Equation (4) expresses the bearing capacity of ring footings N in anisotropic and non-homogeneous clays, with the parameters r_i/r_o, D/r_o, r_e, and $\rho r_o/s_{uTC0}$ corresponding to the geometry of the ring foundation, the embedded depth ratio, the anisotropic strength ratio, and the non-homogeneous behavior of the soil, respectively.

3 Methodology

3.1 Multivariate Adaptive Regression Splines (MARS) model

Recently, MARS has been used to analyze input parameter sensitivity in the settlement of caisson foundation [39], determine the penetration resistance of a spherical penetrometer in clays [40], and solve problems related to lateral displacement of D-wall in excavation and tunneling [41].

MARS model divides data into groups. The boundaries of each group are determined by Knots, using an adaptive regression algorithm, and within each group, a linear regression model is implemented. The regression lines are connected by Knot and expressed by basic functions described in Eq (5).

$$\mathrm{BF} = \max\,(0,\, x-t) = \begin{cases} x-t & \text{if } x \geq t \\ 0 & \text{otherwise} \end{cases} \tag{5}$$

where t is a Knot value and x is an input variable.

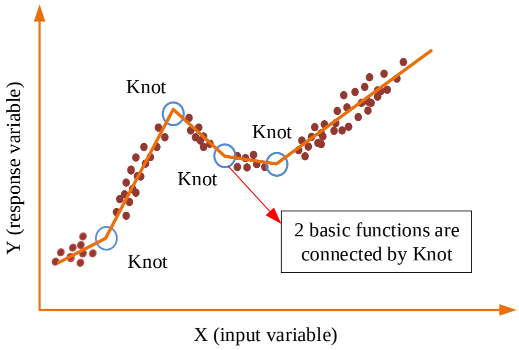

Fig. 4. The idea of MARS model.

It is described in Fig. 5 that MARS algorithm has two main steps. Firstly, it generates many basic functions for the data and then deletes the least effective terms, using a pruning algorithm based on Generalized Cross validation (GCV) [42,43]. Then, it creates an optimal model that can show the nonlinear relationship between input and output variables.

The MARS model combines basic linear functions (BFs) to find the equation that represents the relationship between input and output variables, using Eq. (6). The equation contains a constant a_0, N number of BFs, g_n (the n^{th}BF), and an (n^{th} coefficient of g_n). The accuracy of the MARS model can be enhanced by adding more data sections or basic functions [44-47].

$$f(x) = a_o + \sum_{n=1}^{N} a_n g_n(X) \tag{6}$$

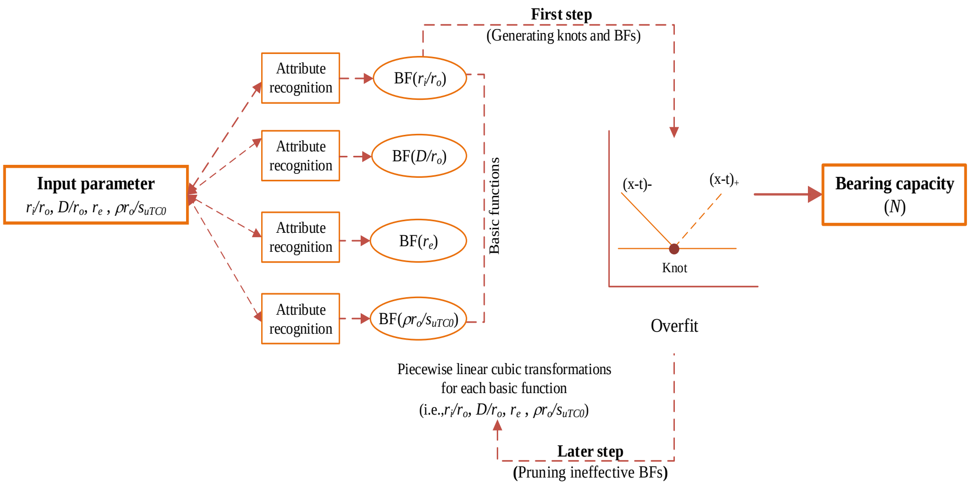

Fig. 5. Two main steps of MARS algorithm.

3.2 Data collection

Previous studies on ring foundation issues and stability analysis in anisotropic clays, such as Lee et al., Remadna, and Lai et al., are the sources of the collected datasets. The datasets comprise 720 investigated cases, covering various combinations of dimensionless input parameters: r_i/r_o=0, 0.25, 0.33, 0.5 and 0.75, D/r_o=0, 0.5, 1 and 2, r_e=0.5, 0.6, 0.7, 0.8, 0.9 and 1, and $\rho r_o/s_{uTC0}$= 0, 1, 2.5, 5, 10 and 15. The input variables and output stability number of all cases were used as training data for the MARS model.

4 Analysis results and new equation

In this research, the MARS model's performance is evaluated by varying the number of BFs and assessing the Root Mean Squared Error (RMSE) and coefficient of determination (R2 value) as statistical measures. The R2 ranges from 0 to 1, and the closer this value is to 1, the better the agreement between the prediction and the target value is. Conversely, an R2 value closer to 0 indicates the opposite. Additionally, the accuracy of the MARS models is also analyzed using the Root Mean Squared Error (RMSE), which measures the error between the prediction and target value. Specifically, a smaller RMSE value indicates a higher accuracy of the model, as determined by the equation provided:

$$RMSE = \sqrt{\frac{1}{n}\sum_{i=1}^{n}(y'_i - y_i)^2} \quad (7)$$

where n is the number of samples, and $(y'_i - y_i)$ is the result of the prediction minus the target.

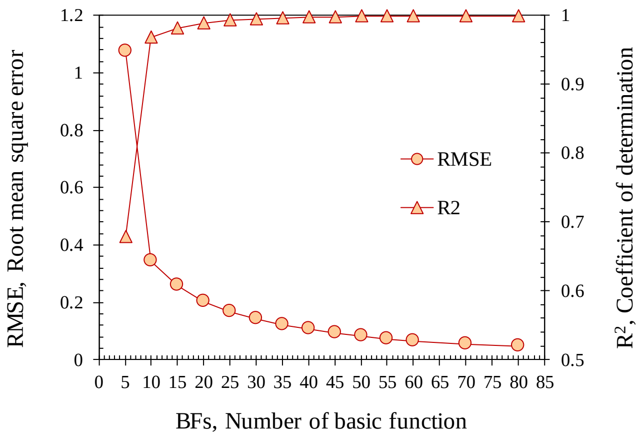

Fig. 6. The variation of RMSE and R2 due to the changing of the number of BF

To begin with, it is illustrated in Fig. 6 that the number of basic functions has an effect on the values of RMSE and R^2. When the number of basic functions increases, the RMSE reduces, and R^2 approaches 1. Besides, the RMSE and R^2 stabilize when the number of basic functions is 35. Therefore, the MARS model with 35 BFs is utilized for further analysis.

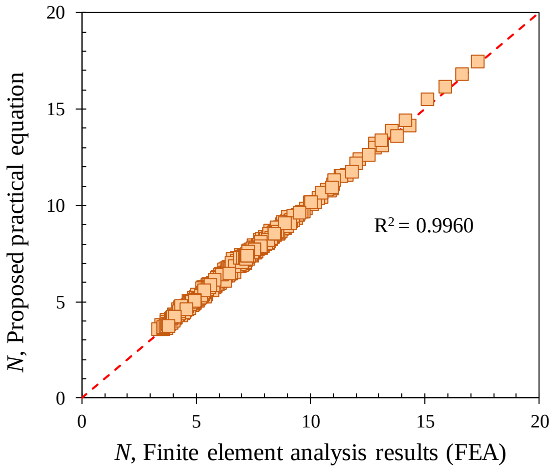

Fig. 7. The comparison between bearing capacity N from the proposed equation and FEA.

Finally, the relationship between the bearing capacity N and input variables is expressed by a new equation in Eq. 8, with the basic function forms listed in Table 1. To verify the proposed equation's accuracy, a comparison between predicted and previous research numbers is performed, as shown in Fig. 7. The results reveal a strong agreement between them, indicating that the proposed equation can be utilized to determine the bearing capacity number of ring foundations in anisotropic and heterogeneous clays while considering a set of parameters above. Note that the proposed equation is an approximation with respect to the parameter values within the investigated range, as detailed in part 3.2, so the results may be unreliable for input values outside the specified range.

$$N = 5.16394 - 2.2991 \times BF1 + 5.82133 \times BF2 + 5.3844 \times BF3 + 0.0197118 \times BF4 - 0.272858 \times BF5 - 0.017462 \times BF6 + 0.678281 \times BF7 + 1.66449 \times BF9 - 0.455259 \times BF11 + 1.0747 \times BF12 - 2.204 \times BF13 + 0.603792 \times BF14 - 0.93508 \times BF15 - 1.31844 \times BF16 - 7.65449 \times BF17 + 1.86525 \times BF18 + 0.0411758 \times BF19 - 2.97063 \times BF20 + 0.903993 \times BF21 + 4.39949 \times BF22 - 1.16772 \times BF23 - 0.640157 \times BF24 - 2.18055 \times BF26 + 0.550908 \times BF28 + 0.484107 \times BF29 - 1.64164 \times BF32 + 3.19047 \times BF33 + 6.84792 \times BF34 - 0.45469 \times BF35 \quad (8)$$

Table 1. New equation and its basic functions

BF	Equation	BF	Equation
BF1	max (0, r_i/r_o – 0.33)	**BF18**	max (0, 0.7 – r_e) × BF2
BF2	max (0, 0.33 –r_i/r_o)	**BF19**	max (0, m – 1) × BF2
BF3	max (0, r_e – 0.5)	**BF20**	max (0, 1 – m) × BF2
BF4	max (0, m – 2.5)	**BF21**	max (0, D/r_o – 0.5) × BF20
BF5	max (0, 2.5 – m)	**BF22**	max (0, 0.5 – D/r_o) × BF20
BF6	max (0, D/r_o – 0.5) × BF4	**BF23**	max (0, r_e – 0.5) × BF8
BF7	max (0, 0.5 – D/r_o) × BF4	**BF24**	max (0, D/r_o – 0.5) × BF1
BF8	max (0, r_i/r_o – 0.25) × BF7	**BF25**	max (0, 0.5 – D/r_o) × BF1
BF9	max (0, 0.25 – r_i/r_o) × BF7	**BF26**	max (0, r_e – 0.7) × BF1
BF10	max (0, D/r_o – 0.5) × BF5	**BF28**	max (0, r_i/r_o – 0.5) × BF10
BF11	max (0, 0.5 – D/r_o) × BF5	**BF29**	max (0, 0.5 – r_i/r_o) × BF10
BF12	max (0, r_i/r_o – 0.33) × BF11	**BF31**	max (0, 0.7 – r_e)
BF13	max (0, 0.33 – r_i/r_o) × BF11	**BF32**	max (0, D/r_o + 0.000000059604)× BF31
BF14	max (0, r_e – 0.7) × BF7	**BF33**	max (0, r_i/r_o – 0.25) × BF32
BF15	max (0, 0.7 – r_e) × BF7	**BF34**	max (0, 0.25 – r_i/r_o) × BF32
BF16	max (0, r_e – 0.5) × BF11	**BF35**	max (0, m – 0) × BF25
BF17	max (0, r_e – 0.7) × BF2		

5 Conclusion

The determination of the bearing capacity *N* of ring foundation in anisotropic and heterogeneous clays has been proposed in this paper, utilizing a new equation based on MARS model. The output results are calculated from 7 designed parameters (r_i, r_o, D, s_{uTC}, s_{uTE}, s_{uDSS}, and ρ), which are transformed into four dimensionless input variables (r_i/r_o, D/r_o, r_e, and m). The predicted values of N demonstrate a significant agreement with the numerical results from previous studies. Additionally, the proposed equation has a potential practical application in predicting the capacity of ring foundations in anisotropic and heterogeneous clays.

Acknowledgment

We acknowledge Ho Chi Minh City University of Technology (HCMUT), VNU-HCM for supporting this study.

References

1. Hataf N, Razavi M (2003) Model tests and finite element analysis of bearing capacity of ring footings on loose sand, Iranian journal of science and technology transaction b- engineering
2. Ohri M, Purhit D, and Dubey M (1997) Behavior of ring footings on dune sand overlaying dense sand. In: Pres International Conference of Civil Engineers, Tehran, Iran
3. Shalaby SI (2017) Bearing capacity of ring footing on stabilized clay with sand trench-stone pile combination. Int J Sci Eng Appl Sci 3(5):218–226
4. Demir A, O¨ rnek M, Laman M, and Yildiz A (2012) Analysis of ring footings using field test results. In: Proc, 3rd Int Conf of New Developments in Soil Mechanics and Geotechnical Engineering
5. Zhao L, Wang J (2008) Vertical bearing capacity for ring footings. Comput Geotech 35(2):292–304
6. Benmebarek S, Remadna M, Benmebarek N, Belounar L (2012) Numerical evaluation of the bearing capacity factor Nc0 of ring footings. Comput Geotech 44:132–138
7. Choobbasti A, Hesami S, Najafi A, Pirzadeh S, Farrokhzad F, et al (2010) Numerical evaluation of bearing capacity and set- tlement of ring footing; case study of Kazeroon cooling towers. Int J Res Rev Appl Sci 4(2):263–271
8. Chavda JT, Dodagoudar G (2021) On vertical bearing capacity of ring footings: finite element analysis, observations and recommendations. Int J Geotech Eng 15(10):1207–1219
9. Kumar J, Chakraborty M (2015) Bearing capacity factors for ring foundations. J Geotech Geoenviron Eng 141(10):06015007
10. Khatri VN, Kumar J (2009) Bearing capacity factor N for a rough conical footing. Geomech Eng 1(3):205–218
11. Lee JK, Jeong S, Lee S (2016) Undrained bearing capacity factors for ring footings in heterogeneous soil. Comput Geotech 75:103–111
12. Yang C, Zhu Z, Xiao Y (2020) Bearing capacity of ring foun- dations on sand overlying clay. Appl Sci 10(13):4675
13. Birid K, Choudhury D (2021) Depth factors for ring foundations in cohesive soil using numerical analysis. Int J Geotech Eng 15(10):1220–1230
14. Yodsomjai W, Keawsawasvong S, Lai VQ (2021) Limit analysis solutions for bearing capacity of ring foundations on rocks using Hoek-Brown failure criterion. Int J Geosyn Ground Eng 7(2):1–10
15. Lai VQ, Shiau J, Keawsawasvong S, and Tran DT (2022) Bearing capacity of ring foundations on anisotropic and heterogenous clays: FEA, NGI-ADP, and MARS. Geotechnical and Geological Engineering: p 1–16

16. Keawsawasvong S, Shiau J, Ngamkhanong C, Qui Lai V, Thongchom C (2022) Undrained stability of ring foundations: axisymmetry, anisotropy, and nonhomogeneity. Int J Geomech 22(1):04021253
17. Casagrande ACN (1944) Shear failure of anisotropic soils. Contrib Soil Mech (BSCE) 1941–1945:122–135
18. Lo KY (1965) Stability of slopes in anisotropic soils. J Soil Mech Found Div 91(4):85–106
19. Ladd C (1991) Stability analysis during staged construction: J Geotech Engng Div ASCE V117, N4, April 1991, P538–615. In: International Journal of Rock Mechanics and Mining Sciences & Geomechanics Abstracts. Pergamon
20. Ladd C and DeGroot D (2003) Recommended practice for soft ground site characterization: Arthur Casagrande Lecture. 12th PCSMGE, MIT, Cambridge, Massachusetts
21. Krabbenhoft K, Lyamin A (2015) Generalised Tresca criterion for undrained total stress analysis. Geotech Lett 5(4):313–317
22. Ukritchon B, Wongtoythong P, Keawsawasvong S (2018) New design equation for undrained pullout capacity of suction caissons considering combined effects of caisson aspect ratio, adhesion factor at interface, and linearly increasing strength. Appl Ocean Res 75:1–14
23. Keawsawasvong S, Ukritchon B (2019) Undrained basal stability of braced circular excavations in non-homogeneous clays with linear increase of strength with depth. Comput Geotech 115:103180
24. Keawsawasvong S, Lai VQ (2021) End bearing capacity factor for annular foundations embedded in clay considering the effect of the adhesion factor. Int J Geosyn Ground Eng 7(1):1–10
25. Keawsawasvong S, Shiau J (2021) Instability of boreholes with slurry. Int J Geosyn Ground Eng 7(4):1–11
26. Keawsawasvong S, Shiau J (2022) Stability of active trapdoors in axisymmetry. Undergr Space 7(1):50–57
27. Seehavong S, Keawsawasvong S (2021) Penetration and uplift resistances of two interfering pipelines buried in clays. Int J Compu Mat Sci Eng 10(04):2150020
28. Keawsawasvong S (2021) Bearing capacity of conical footings on clays considering combined effects of anisotropy and non-ho- mogeneity. Ships and Offshore Structures, p 1–12
29. Rao P, Wu J, Mo Z (2020) 3D Limit analysis of the transient stability of slope during pile driving in nonhomogeneous and anisotropic soil. Adv Civ Eng 7560219
30. Haghsheno H, Arabani M (2021) Seismic bearing capacity of shallow foundations placed on an anisotropic and nonhomoge- neous inclined ground. Indian Geotechn J 51(6):1319–1337
31. Keawsawasvong S, Ukritchon B (2021) Undrained stability of plane strain active trapdoors in anisotropic and non-homogeneous clays. Tunn Undergr Space Technol 107:103628
32. Shiau J, Hassan MM (2021) Numerical investigation of undrained trapdoors in three dimensions. Int J Geosyn Ground Eng 7(2):1–12
33. Lai VQ, Banyong R, Keawsawasvong S (2022) Undrained sinkhole collapse in anisotropic clays. Arab J Geosci 15(8):1–13
34. Ukritchon B, Keawsawasvong S (2019) Three-dimensional lower bound finite element limit analysis of an anisotropic undrained strength criterion using second-order cone programming. Comput Geotech 106:327–344
35. Ukritchon B, Keawsawasvong S (2020) Undrained lower bound solutions for end bearing capacity of shallow circular piles in non-homogeneous and anisotropic clays. Int J Numer Anal Meth Geomech 44(5):596–632

36. Nguyen DK, Nguyen TP, Keawsawasvong S, Lai VQ (2022) Vertical uplift capacity of circular anchors in clay by considering anisotropy and non-homogeneity. Transp Infrastruct Geotechnol 9(5):653–672
37. Keawsawasvong S, Yoonirundorn K, Senjuntichai T (2021) Pullout capacity factor for cylindrical suction caissons in aniso- tropic clays based on anisotropic undrained shear failure criterion. Transp Infrastruct Geotechnol 8(4):629–644
38. 74. Butterfield R (1999) Dimensional analysis for geotechnical engineers. Geotechnique 49(3):357–366
39. Lai, F., Zhang, N., Liu, S., Sun, Y., Li, Y. (2021): Ground movements induced by installation of twin large diameter deeply–buried caissons: 3D numerical modeling. Acta Geotech , 16, 2933–2961
40. Wu, L., Fan, J. (2019): Comparison of neuron–based, kernel–based, tree–based and curve–based machine learning models for predicting daily reference evapotranspiration. PLoS ONE,14, e0217520
41. 37. Raja, M.N.A., Shukla, S.K. (2021): Multivariate adaptive regression splines model for rein-forced soil foundations. Geosynth. Int, 28, 368–390
42. Sirimontree, S., Jearsiripongkul, T., Lai, V.Q., Eskandarinejad, A., Lawongkerd, J., Seehavong, S., Thongchom, C., Nuaklong, P. and Keawsawasvong, S. (2022): Prediction of Penetration Resistance of a Spherical Penetrometer in Clay Using Multivariate Adaptive Regression Splines Model. Sustainability, 14(6), p.3222
43. Caraka, R.E., Chen, R.C., Bakar, S.A., Tahmid, M., Toharudin, T., Pardamean, B. (2020): Employ-ing Best Input SVR Robust Lost Function with Nature–Inspired Metaheuristics in Wind Speed Energy Forecasting. IAENG Int. J. Comput. Sci. 2020, 47, 572–584
44. Sirimontree, S., Jearsiripongkul, T., Lai, V.Q., Eskandarinejad, A., Lawongkerd, J., Seehavong, S., Thongchom, C., Nuaklong, P. and Keawsawasvong, S. (2022): Prediction of Penetration Resistance of a Spherical Penetrometer in Clay Using Multivariate Adaptive Regression Splines Model. Sustainability, 14(6), p.3222
45. Thira Jearsiripongkul., Van Qui Lai., Suraparb Keawsawasvong., Thanh Son Nguyen., Chung Nguyen Van., Chanachai Thongchom and Peem Nuaklong.: Prediction of Uplift Capacity of Cylindrical Caissons in Anisotropic and Inhomogeneous Clays Using Multivariate Adaptive Regression Splines, Sustainability 2022, 14, 4456. https://doi.org/10.3390/su14084456
46. Yodsomjai, W., Lai, V. Q., Banyong, R., Chauhan, V. B., Thongchom, C., & Keawsawasvong, S. (2022) A machine learning regression approach for predicting basal heave stability of braced excavation in non–homogeneous clay. Arabian Journal of Geosciences, 15(9), 1–14
47. Shiau, J. Lai, V. Q., Keawsawasvong, S. Multivariate adaptive regression splines analysis for 3D slope stability in anisotropic and heterogenous clay. Journal of Rock Mechanics and Geotechnical Engineering, Accepted